



Article

Mortality Associated with Extreme Heat in Washington State: The Historical and Projected Public Health Burden

Logan Arnold ^{1,*}, Mark D. Scheuerell ² and Tania Busch Isaksen ^{1,3}¹ Quantitative Ecology and Resource Management, University of Washington, Seattle, WA 98195, USA² U.S. Geological Survey Washington Cooperative Fish and Wildlife Research Unit, School of Aquatic and Fishery Sciences, University of Washington, Seattle, WA 98195, USA³ Department of Environmental and Occupational Health Sciences, University of Washington, Seattle, WA 98195, USA

* Correspondence: larnold3@uw.edu

Abstract: Extreme heat is one of the most important pathways illustrating the connection between climate and human health, and climate change is expected to exacerbate this public health issue. This study first used a case-crossover analysis to characterize the historical (1980–2018) association between summertime heat and non-traumatic mortality in Washington State. A separate analysis was conducted for each of the state’s ten climate divisions to produce distinct exposure–response curves expressing odds of mortality as a function of humidex. Stratified analyses were used to assess the impact of age, sex, race/ethnicity, and select causes of death, and the reported results are pooled across all divisions using meta-analysis. The historical heat–mortality relationship was combined with climate projections to estimate the impact of climate change on heat-related deaths in 2030, 2050, and 2080 under two warming scenarios. The odds ratio (OR) and 95% confidence intervals of mortality at the 99th percentile of humidex compared to the 50th percentile did not include the null value in four climate divisions (E Olympic Cascade Foothills, NE Olympic San Juan, Northeastern, and Puget Sound Lowlands). The statewide odds of mortality are 8% higher (6%, 10%) on 99th percentile days compared to 50th percentile days, driven primarily by an OR of 1.09 (1.06, 1.11) in the Puget Sound Lowlands. Risk is higher for women than men and for Blacks than Whites. Risk increases with age and for diabetic, circulatory, cardiovascular, ischemic, cerebrovascular, and respiratory deaths. The 95% confidence intervals of projected heat-attributable mortality did not overlap with zero in three climate divisions (E Olympic Cascade Foothills, NE Olympic San Juan, and Puget Sound Lowlands). In these three divisions, the average percent increase in heat-attributable mortality across both warming scenarios is 35%, 35%, and 603% in 2030, 2050, and 2080, respectively. This research is the most extensive study of heat-related mortality in Washington to date and can help inform public health initiatives aiming to improve present and future health outcomes in the state.

Keywords: heat-related mortality; case-crossover analysis; climate change; extreme heat; public health; climate divisions



Citation: Arnold, L.; Scheuerell, M.D.; Busch Isaksen, T. Mortality Associated with Extreme Heat in Washington State: The Historical and Projected Public Health Burden. *Atmosphere* **2022**, *13*, 1392. <https://doi.org/10.3390/atmos13091392>

Academic Editors: Alfredo Rocha and Mónica Rodrigues

Received: 12 June 2022

Accepted: 2 August 2022

Published: 30 August 2022

Publisher’s Note: MDPI stays neutral with regard to jurisdictional claims in published maps and institutional affiliations.



Copyright: © 2022 by the authors. Licensee MDPI, Basel, Switzerland. This article is an open access article distributed under the terms and conditions of the Creative Commons Attribution (CC BY) license (<https://creativecommons.org/licenses/by/4.0/>).

1. Introduction

The human body responds to extreme heat by increasing cardiovascular demand in an attempt to provide physiologic cooling and maintain thermal homeostasis, and a failure to meet this demand can lead to a variety of illnesses or death [1]. Epidemiological studies of the association between heat and mortality primarily conclude that abnormally high temperatures are associated with excess mortality and that the exposure–response function is nonlinear, typically described by a V-, U-, or J-shaped curve [2,3]. This relationship has been observed in locations with diverse climates and cultures, including the United States [4–10], Europe [11–13], Latin America [14], India, specifically [15] and South Asia, generally [16], China [17], Russia [18] Australia [19], South Africa [20], and the Middle East and North Africa [21].

Deaths attributed specifically to heat often underestimate the true public health burden of high temperatures [1]. Other commonly identified risk factors include cardiovascular diseases [6,8,12,13,22], respiratory diseases [12,15], diabetes [8,12,23], age [4,8,11,14,15], and lack of access to air conditioning [5,6,22,24,25]. (Systemic) racism produces different health outcomes for racially defined groups [26,27], including in the context of heat-related mortality [23,24,28], as communities of color often have reduced access to air conditioning [25] and live disproportionately in areas most susceptible to the urban heat island effect [29]. Although the most recent IPCC Working Group 6 report summarized with very high confidence that geographical differences in heat-related mortality will be driven by “growth in regions with tropical and subtropical climates” [30], it is well-documented that temperate regions, such as Washington State, are more sensitive to heat events, perhaps due to less appreciation of risk, lower prevalence of air conditioning, or weaker physiologic acclimatization [4–6,9,31–33]. With average global temperatures predicted to continue increasing [34], along with the frequency, length, and intensity of future extreme heat events [35], risk estimates that better characterize the full heat-health burden will be important as public health practitioners pursue equitable future health outcomes.

Washington State, an area largely characterized by a historically temperate climate and a relatively low prevalence of air conditioning, is an important location for research into heat-related health outcomes. Jackson et al. [36] examined four areas in Washington State and obtained relative risk values in the greater Seattle area that indicated a significant relationship between heat event duration and increased daily mortality rates for non-traumatic deaths in persons aged 45 and above. Although results in the other three areas were not statistically significant, the patterns of elevated relative risk estimates suggest that there is also a real difference in mortality rates during heat events in these areas; however, sample size issues prevented statistically significant estimates. Busch Isaksen et al. [7] computed a 1.83% (95% CI: 0.77%, 2.91%) increase in mortality for all ages, all non-traumatic mortality in King County for each one degree change in humidex above the optimal alert threshold of 35.7 humidex. A subsequent analysis [8] also found a 10% increase (95% CI: 6%, 14%) in the risk of death on a heat day versus a non-heat day for all ages, all causes.

The Pacific Northwest historically has experienced few severe heatwaves, but climate models suggest that this area will become increasingly susceptible to extreme heat events [35] and that it may experience greater summertime warming due to climate change than most of the rest of the continental United States [37]. Thus, a region that is already vulnerable to heat may soon face a climate to which it is not adapted nor acclimated, as illustrated by the June/July 2021 record-breaking “heat dome” that resulted in elevated hospitalizations and mortality throughout Oregon, Washington, and southwest Canada. Jackson et al. [36] found that projected non-traumatic deaths due to heat days in the Seattle region were greatest for people in the 65+ age group in all years and warming scenarios analyzed, although the results for the rest of the state were not statistically significant. In King County, Busch Isaksen et al. [7] identified the 85+ age group as being most at-risk of heat-related mortality in a changing climate.

Previous studies in Washington State have assessed exposure using average maximum daily humidex averaged at the county-level [7,8,36]. This is an important limitation, given that there is significant spatial variation in heat across any given county. Exposure variation is further illustrated by the fact that many counties in Washington have more than one climatic zone within their geopolitical boundaries. This study addresses the potential exposure misclassification when using average county-level humidex by assigning average daily maximum humidex exposure at the individual level. Additionally, this study improves heat-risk estimates by spatially aggregating risk to the climate zone level, rather than a geopolitical county level, thereby increasing power to observe effects in the more rural parts of the state, while recognizing individuals adapt to their climatic conditions [6]. Finally, this study provides the most up-to-date statewide characterization of observed and predicted heat-mortality risk. Previous results have been used to inform risk communication

campaigns and to drive public health intervention planning. This updated work is widely anticipated by our practice community.

This study uses a case-crossover approach to investigate the heat–mortality relationship in Washington State and explores possible heterogeneity in the dose–response curve across the state’s ten climate divisions, as defined by the National Oceanic and Atmospheric Administration (NOAA, [38]). The impact of heat on mortality is assessed for all ages and all causes in addition to possible effect modification by age, sex, race/ethnicity, and cause of death. Pooled odds ratio (OR) estimates and 95% confidence intervals (CIs) are reported, comparing the odds of mortality at the 99th percentile of summertime humidex to the 50th percentile. The historical results are also combined with climate projections to investigate the impact that climate change will have on excess mortality attributable to extreme heat.

2. Materials and Methods

2.1. Data Sources

2.1.1. Mortality Data

Mortality data from the Washington State Department of Health covers the entire state and the years 1980–2018. Only deaths during the months of May through September were included in the analysis, resulting in 153 days/calendar year and 5967 days for the entire study period. Non-traumatic mortality across all ages was the primary outcome of interest (ICD-9: 0–799; ICD-10: A00–R99). Investigations of specific subsets of all-cause mortality were determined a priori based on existing literature [7,8,36] and included diabetes (ICD-9: 250; ICD-10: E08–E13), circulatory (ICD-9: 390–459; ICD-10: I00–I99, G45, G46), cardiovascular (ICD-9: 393–429; ICD-10: I05–I52), ischemic (ICD-9: 410–414; ICD-10: I20–I25), cerebrovascular (ICD-9: 430–438; ICD-10: I67), respiratory (ICD-9: 460–519; ICD-10: J00–J99), nephritis and nephrotic syndromes (ICD-9: 580–589; ICD-10: N17–N19), acute renal failure (ICD-9: 584; ICD-10: N17), and mental disorders (ICD-9: 290–316; ICD-10: F01–F69). Other individual-level characteristics include age (divided into six age groups: 0–4, 5–14, 15–44, 45–64, 65–84, and 85+), sex, and race/ethnicity, as defined by the Washington State Department of Health. Each death had an associated latitude and longitude value, enabling aggregation of cases into one of the ten climate divisions in Washington [38], depicted in Figure 1.

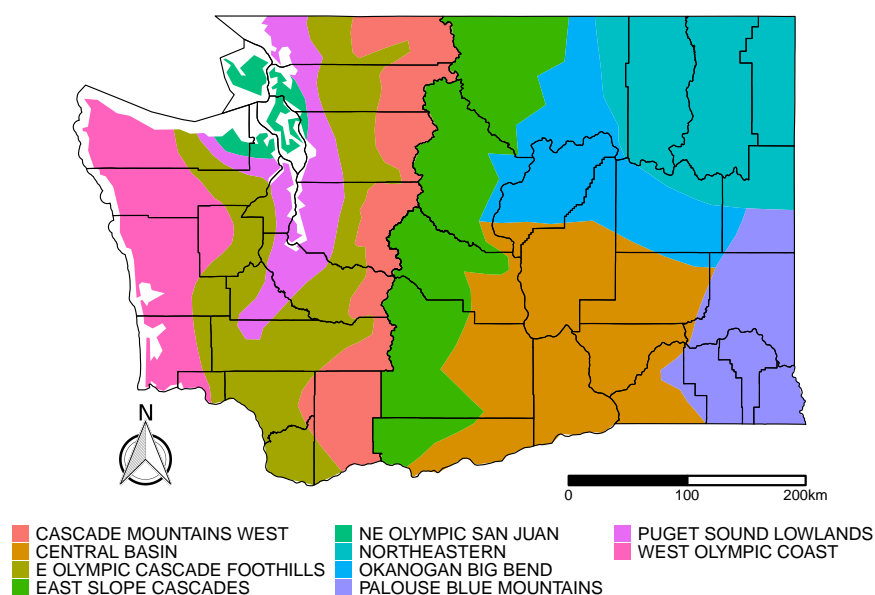


Figure 1. Map of NOAA climate divisions in Washington.

2.1.2. Historical Meteorological Data

The gridMET data [39] from the University of California Merced Climatology Lab [40] were used to obtain historical meteorological data (daily temperature and relative humidity

values) to characterize exposure to heat. These data, which are intended to be used in ecological applications and modeling, were produced using a hybrid method that combines temporally rich data from the North American Land Data Assimilation System Phase 2 (NLDAS, [41]) with spatially rich data from the Parameter-elevation Regressions on Independent Slopes Model (PRISM, [42]). The gridMET data have observations at a spatial resolution of 1/24 degree ($\sim 4 \text{ km} \times 4 \text{ km}$) and were validated using weather stations in the western United States [39].

2.1.3. Climate Projections

The Multivariate Adaptive Constructed Analogs (MACA, [43]) statistical downscaling of 20 global circulation models (GCMs) of the Coupled Model Inter-Comparison Project 5 (CMIP5) from the University of California Merced Climatology Lab [44] were used to obtain projected meteorological data for the years 2030, 2050, and 2080. The projected meteorological data, like the historical data, have a resolution of $\sim 4 \text{ km} \times 4 \text{ km}$ and were validated using reanalysis across the western United States. Although the MACA downscaling method was originally developed to produce climate projections to use in wildfire applications, these data have been used previously to forecast heat-related deaths [45]. Indeed, MACA is quite useful in heat epidemiology because it produces projected, daily values for not only temperature, but also humidex on a spatial resolution that minimizes exposure misclassification when compared to regional or global climate projections [43].

To account for uncertainty in future greenhouse gas emissions, two representative concentration pathway (RCP) scenarios were used to represent intermediate (RCP4.5) and worst-case (RCP8.5) trajectories. For each combination of year and RCP, the results from all 20 models were averaged to obtain a single projected temperature and relative humidity value for every grid point and every day from 1 May–31 September.

2.2. Exposure Assessment

For both the historical and projected analyses, temperature and relative humidity values were combined to construct the exposure metric, daily maximum humidex. Humidex is a unitless apparent temperature measurement that incorporates both air temperature and humidity [46]:

$$\text{Humidex} = T + \frac{5}{9}(v - 10) \quad (1)$$

where T is the air temperature ($^{\circ}\text{C}$), $v = (6.112 \times 10^{\frac{7.5T}{237.7+T}}) \frac{H}{100}$ is the vapor pressure (kPa), and H is the relative humidity (%). Humidex was chosen because it incorporates humidity, which is known to influence the physiological response to extreme heat [1,47], and for comparison to previous studies, particularly those in the Pacific Northwest [7,8,36], that also utilize humidex as the exposure metric. A nearest neighbors calculation was used to assign individual-level humidex exposure by comparing the latitude and longitude of death to the gridded meteorological data. The projected humidex values were also calibrated to the historical data to correct for climate model biases [48].

2.3. Case-Crossover Analysis for the Historical Period

The case-crossover study design [49] was used to quantify the historical (1980–2018) relationship between humidex and mortality. A case-crossover study design is akin to the traditional matched case-control design because selection is based on the outcome; however, like a crossover study, each case serves as its own control. Risk of mortality is inferred by comparing a person's exposure to humidex on the date of death to multiple control or "referent" periods [50], and matching each case to itself eliminates confounding by constant or slowly varying individual characteristics, such as age and sex [49]. Control days were selected by matching the date of death to all other days that share the same day of week, month, and year of the death. This approach has been used extensively in previous

heat-related mortality studies [11–14,19] and is ideal because it controls for seasonality, long-term trends, and any potential effects related to the day of the week by design [51].

A conditional logistic regression model was created for each climate division in Washington. To model the nonlinear relationship between heat and mortality, both polynomials and natural cubic splines were used to incorporate individual-level humidex as a continuous variable. Akaike information criterion (AIC) was used for model selection, and ultimately a quadratic polynomial was chosen to produce an exposure–response curve that describes the odds of mortality at all humidex values:

$$P(Y_{il} = 1|X_{il}) = \frac{\exp(\alpha_i + \beta_1 * X_{il} + \beta_2 * X_{il}^2)}{1 + \exp(\alpha_i + \beta_1 * X_{il} + \beta_2 * X_{il}^2)} \quad (2)$$

where $P(Y_{il})$ is that probability on day l that person i is a case ($Y_{il} = 1$), given the humidex values that person i experienced on day l (X_{il}). The odds of mortality at a specific humidex value are therefore given by:

$$\exp(\beta_1 * X_{il} + \beta_2 * X_{il}^2) \quad (3)$$

To ease the interpretation of model results, the odds of mortality at the 99th percentile of humidex were compared to the odds at the 50th percentile to create a single odds ratio (OR), by climate division. Stratified analyses were conducted to explore effect modification by both age and cause of death. For both the full and stratified analyses, the ORs in each climate division were pooled using fixed-effects meta-analysis to obtain a single, state-level estimate.

All analyses were conducted using R 3.6.2 [52]. Conditional logistic regression was implemented with the survival package [53], whereas the meta package [54] was used for meta-analysis.

2.4. Projected Heat-Attributable Deaths Due to Climate Change

Calculations for projected heat-related deaths were guided by Vicedo-Cabrera, Sera, and Gasparrini [55]. Specifically, it was assumed that populations and outcome rates will remain constant in the future. This approach is likely unrealistic, as it neglects time-varying characteristics, such as age structure and access to air conditioning, that influence the occurrence of heat-related health outcomes, but it isolates the effect of climate from these other important trends to answer the question, “How would the current population respond if exposed to warmer temperatures projected in the future?”

First, the number of deaths attributable to heat above the 99th percentile in each climate division were calculated for the historical period using the following formula (adapted from Equation (2) in [55]):

$$D_{\text{attr}} = D \times (1 - e^{-\beta H}) \quad (4)$$

where D is the total number of deaths occurring on days above the 99th percentile of humidex and $(1 - e^{-\beta H})$ is the fraction of deaths attributable to (a quadratic function of) humidex, H , restricted to humidex values above the 99th percentile; β corresponds to the coefficients of the exposure–response curve derived in the case-crossover analysis. (Note that this formula reduces to $\frac{RR-1}{RR}$ in the case of a linear or binary relationship).

After obtaining the number of deaths attributable to extreme heat in the historical period, projected, individual-level humidex values were assigned to each death in the years 2030, 2050, and 2080 and under the emissions scenarios RCP4.5 and RCP8.5 based on the grid point in which the death is located. Next, Equation (4) was applied using the historical 99th percentile of humidex in each climate division as a cutoff to calculate the projected public health burden. The results of the projected heat-attributable death calculations are reported as percent increases over the historical period.

3. Results

3.1. Historical Public Health Burden

Non-traumatic mortality counts broken down by age, sex, race/ethnicity, and cause of death are given in Table 1 for Washington and each climate division. In total, 563,365 deaths were included in the analysis. Of these deaths, 56% of them occurred in the Puget Sound Lowlands, the division in which the majority of Seattle, Washington's most populous city, is located. The range of deaths in each climate division is very large, with only 0.18% of deaths occurring in the least populous division, the Cascade Mountains West. The two largest age groups are 65–84 (48.0%) and 85+ (29.7%), respectively. The distribution across sexes is fairly equal, although more women than men are included in the data (50.7% vs. 49.3%). White individuals are by far the largest racial/ethnic category (92.1%), and the vast majority of non-White deaths are in the Puget Sound Lowlands.

Table 2 shows the distribution of humidex during the historical period in each of the climate divisions. The distribution of humidex, like the distribution of mortality, is also quite variable across climate divisions. There is a 26% difference between the climate division with the lowest median humidex value (West Olympic Coast) to the division with the highest median humidex value (Central Basin). Similarly, there is a 20% difference in the 99th percentiles of humidex between these two climate divisions. Multiple pairwise *t*-tests using the Bonferroni correction were conducted to assess humidex heterogeneity across all climate divisions at the $\alpha = 0.05$ level, and the only two that were identified as having the same mean were East Slope Cascades and Puget Sound Lowlands. However, these two divisions are not adjacent and consequently could not be combined.

Figure 2 shows the humidex–mortality exposure–response function for each climate division. The function describes the odds of mortality (and 95% CI) at each humidex value, with the horizontal dashed line indicating the null value of 1.0. The vertical dashed lines denote the 50th and 99th percentiles of humidex for that climate division. Despite humidex distributions that vary from one climate division to another, the dose–response curves in Figure 2 are quite similar, and all generally resemble a J- or U-shape. Excluding the Cascade Mountains West division, which had the fewest number of deaths during the study period (1020), the qualitative value for the estimated odds of mortality at the 99th percentile of humidex is quite similar across all climate divisions. The most notable difference is in the associated 95% CI: it is quite tight and mostly non-overlapping with the null value in the East Olympic Cascade Foothills, NE Olympic San Juan, Northeastern, and Puget Sound Lowlands regions but frequently overlaps with the null value in the other six climate divisions. In all regions, the estimated function becomes less precise moving away from the 50th and, especially, 99th percentiles.

Figure 3 is a forest plot depicting ORs (and 95% CIs) of mortality, comparing the 50th and 99th percentiles of humidex, for each climate division as well as a single, statewide value produced via meta-analysis. All climate divisions had point estimates above 1.00, but only four (E Olympic Cascade Foothills, NE Olympic San Juan, Northeastern, and Puget Sound Lowlands) had CIs that did not overlap with the null value. The pooled OR was 1.08 (1.06, 1.10), indicating that odds of mortality are 8% (6%, 10%) higher on days at the 99th percentile of humidex than on days at the 50th percentile of humidex for the entire state of Washington. This value was driven primarily by an OR of 1.09 (1.06, 1.11) in the Puget Sound Lowlands.

Table 1. Non-traumatic mortality characteristics.

Characteristic	All	Climate Division									
		Cascade Mountains West	Central Basin	E Olympic Cascade Foothills	E Slope Cascades	NE Olympic San Juan	Northeastern	Okanogan Big Bend	Palouse Blue Mountains	Puget Sound Lowlands	West Olympic Coast
Total	563,365	1020	62,794	85,498	4329	14,711	52,685	6479	7155	316,999	11,695
Age											
0–4	7133	13	1033	810	42	88	636	52	59	4311	89
5–14	970	-	118	141	-	-	91	12	-	569	12
15–44	18,948	35	2006	2599	94	233	1575	158	176	11,800	272
45–64	98,702	233	10,393	15,996	775	1838	8914	1109	1059	56,145	2240
65–84	270,513	514	30,422	42,247	2174	7240	25,592	3279	3449	149,498	6098
85+	167,090	222	18,822	23,704	1236	5302	15,876	1868	2406	94,670	2984
Sex											
Female	285,395	452	31,588	42,359	1982	7366	26,836	3148	3596	162,397	5671
Male	277,955	568	31,204	43,137	2347	7345	25,848	3331	3559	154,592	6024
Race/Ethnicity											
White	518,873	997	57,769	82,544	4241	14,321	50,758	6078	6902	284,114	11,149
Black	14,429	-	701	592	-	37	572	23	21	12,433	40
Asian	12,341	-	326	700	-	106	324	17	37	10,780	42
Native American	6058	11	923	669	26	122	663	288	30	2,983	343
Hispanic	5980	-	2842	400	36	47	74	56	17	2454	49
Native Hawaiian or Other Pacific Islander	4296	-	106	392	-	33	139	-	-	3571	43
Cause of Death											
Diabetes	10,004	20	1276	1576	64	226	919	140	132	5427	224
Circulatory	213,937	335	25,109	31,318	1607	5380	20,184	2434	2760	120,153	4657
Cardiovascular	160,118	261	18,970	23,972	1215	3970	14,822	1813	2005	89,483	3607
Ischemic	102,827	148	13,129	15,296	839	2528	9731	1236	1290	56,218	2412
Cerebrovascular	19,905	16	2367	2480	121	373	1919	194	273	11,802	360
Respiratory	54,393	92	5894	8375	395	1398	5716	657	758	29,845	1263
Nephritis and nephrotic	4160	-	513	552	22	78	417	46	72	2371	82
Acute Renal Failure	684	-	81	96	-	-	69	-	16	394	-
Mental Disorders	12,108	23	1146	1938	86	269	1013	143	165	7099	226

‘-’ denotes less than 10 observations.

Table 2. Historical humidex descriptive statistics.

Climate Division	Humidex (1980–2018)								
	Mean	SD	Min	Max	25th	50th	75th	95th	99th
Cascade Mountains West	22.74	6.82	1.23	41.36	17.80	22.91	27.78	33.51	36.77
Central Basin	27.24	6.55	5.66	48.40	22.53	27.50	32.11	37.56	40.56
E Olympic Cascade Foothills	24.97	6.39	−1.29	48.14	20.40	24.97	29.44	35.55	39.57
E Slope Cascades	23.43	6.69	1.43	42.24	18.65	23.70	28.38	33.98	37.16
NE Olympic San Juan	21.77	4.70	6.11	39.30	18.53	21.71	24.93	29.72	32.87
Northeastern	24.70	6.71	2.85	44.92	19.79	24.99	29.73	35.25	38.01
Okanogan Big Bend	25.49	6.65	3.48	46.08	20.66	25.68	30.45	36.03	39.14
Palouse Blue Mountains	25.19	6.85	3.91	44.78	20.25	25.56	30.28	35.83	38.84
Puget Sound Lowlands	23.50	5.91	5.57	46.44	19.26	23.46	27.64	33.42	36.98
West Olympic Coast	21.29	4.61	5.88	44.83	18.31	21.20	24.03	29.21	33.77

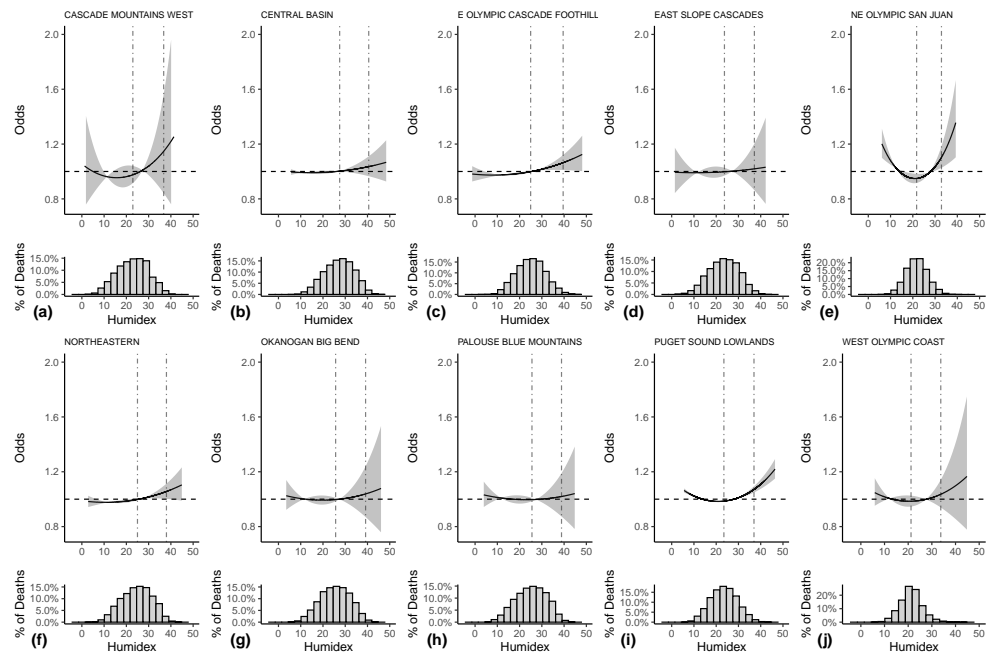


Figure 2. Humidex–mortality exposure–response curves for each of Washington’s climate divisions: (a) Cascade Mountains West, (b) Central Basin, (c) E Olympic Cascade Foothills, (d) East Slope Cascades, (e) NE Olympic San Juan, (f) Northeastern, (g) Okanogan Big Bend, (h) Palouse Blue Mountains, (i) Puget Sound Lowlands, and (j) West Olympic Coast.

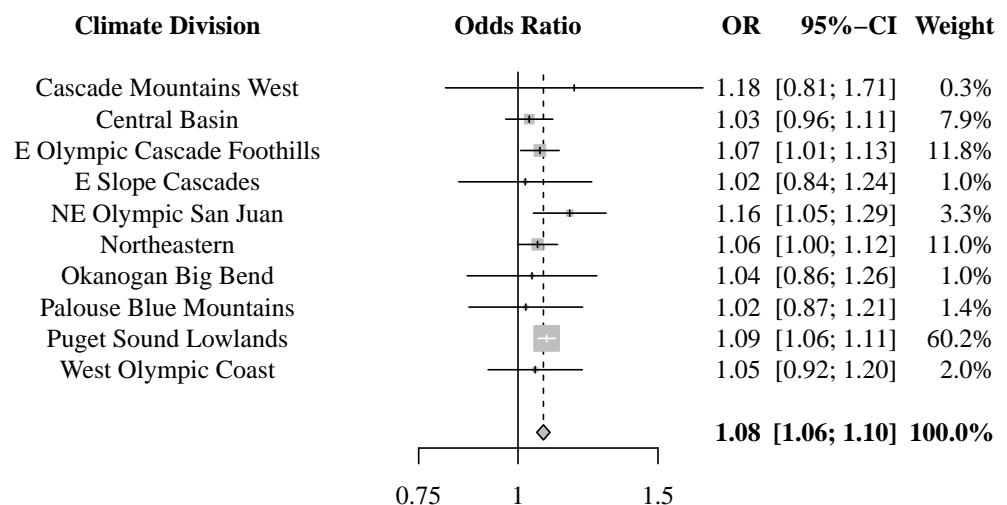


Figure 3. Odds ratio and 95% CI of mortality, comparing the 99th and 50th percentiles of humidex.

The results for effect modification by age, sex, and race/ethnicity are given in Table 3 and by both age and cause of death in Table 4. All values represent ORs pooled across

all ten climate divisions. The OR for non-traumatic mortality increases with age, with the 85+ age group at greatest risk of non-traumatic mortality during a heat event. The point estimate is higher for females than males as well as for Blacks than Whites, though the confidence intervals overlap somewhat. The pooled OR was not significant for other racial/ethnic categories. Diabetic, circulatory, cardiovascular, ischemic, cerebrovascular, and respiratory deaths all have 95% CIs that are non-overlapping with 1. With the exception of diabetic and cerebrovascular deaths, the OR for cause-specific mortality also increases with age; both diabetic deaths and cerebrovascular deaths only have a significant OR for the 65–84 age group. We also explored effect modification by multiple variables, e.g., by both race and age, but many of these investigations yielded wide confidence intervals due to small sample sizes. Comprehensive effect modification results can be found in the Supplementary Materials.

Table 3. Odds ratio (95% CI) of non-traumatic mortality comparing the 99th and 50th percentiles of humidex, by age group, sex, and race/ethnicity.

Group	Observations (%)	OR (95% CI)
Total	563,365 (100)	1.08 (1.06, 1.10)
Age		
0–4	7133 (1.3)	0.90 (0.75, 1.08)
5–14	970 (0.2)	0.90 (0.56, 1.45)
15–44	18,948 (3.4)	1.05 (0.94, 1.17)
45–64	98,702 (17.5)	1.06 (1.02, 1.12)
65–84	270,513 (48.0)	1.07 (1.04, 1.10)
85+	167,090 (29.7)	1.09 (1.06, 1.13)
Sex		
Female	285,395 (50.7)	1.08 (1.05, 1.11)
Male	277,955 (49.3)	1.06 (1.03, 1.09)
Race/Ethnicity		
White	518,873 (92.1)	1.07 (1.05, 1.09)
Black	14,429 (2.6)	1.15 (1.02, 1.30)
Asian	12,341 (2.2)	1.06 (0.93, 1.21)
Native American	6058 (1.1)	1.08 (0.89, 1.32)
Hispanic	5980 (1.1)	1.01 (0.84, 1.21)
Native Hawaiian or Other Pacific Islander	4296 (0.8)	0.97 (0.77, 1.20)

Results are pooled across all climate divisions using fixed-effects meta-analysis. Bold rows indicate 95% CIs that did not include 1.

3.2. Projected Public Health Burden

Figure 4 shows maps of projected humidex anomalies (projected values minus historical values) in Washington for 2030, 2050, and 2080 under both RCP4.5 and RCP8.5. In 2030, the difference between projected and historical humidex values is less than 2 for most of the state under both RCPs. By 2050, the two RCPs start to produce divergent results. Warming remains somewhat modest under RCP4.5, and very few parts of the state have projected humidex anomalies exceeding 4. Conversely, most of the state exceeds this threshold in 2050 under RCP8.5. This discrepancy continues in 2080; most projected humidex anomalies are between 4 and 6 under RCP4.5, whereas the humidex anomalies are between 8 and 10 for the entire state under RCP8.5.

The total number of deaths attributable to heat during the historical period (1980–2018) and the percent increase in 2030, 2050, and 2080 under RCP4.5 and RCP8.5 are given in Table 5. Only three climate divisions—E Olympic Cascade Foothills, NE Olympic San Juan, and Puget Sound Lowlands—had 95% CIs for the percent increase over the historical period that did not overlap with 0; in these three zones, the CI did not include 0 in any year or under either RCP.

Table 4. Odds ratio (95% CI) of non-traumatic mortality comparing the 99th and 50th percentiles of humidex, by age group and cause of death.

Cause of Death (Total Cases)	All Ages	0–4	5–14	15–44	45–64	65–84	85+
All Non-Traumatic Causes (563,365)	1.08 (1.06, 1.10)	0.90 (0.75, 1.08)	0.90 (0.56, 1.45)	1.05 (0.94, 1.17)	1.06 (1.02, 1.12)	1.07 (1.04, 1.10)	1.10 (1.06, 1.13)
Diabetes (10,004)	1.20 (1.03, 1.39)	NA	NA	1.25 (0.60, 2.63)	1.12 (0.81, 1.56)	1.25 (1.03, 1.52)	1.12 (0.80, 1.56)
Circulatory (213,937)	1.10 (1.07, 1.14)	1.10 (0.40, 3.01)	0.68 (0.10, 4.71)	1.08 (0.86, 1.35)	1.09 (1.00, 1.19)	1.09 (1.04, 1.15)	1.11 (1.05, 1.17)
Cardiovascular (160,118)	1.10 (1.06, 1.14)	1.36 (0.45, 4.14)	0.30 (0.02, 3.56)	1.12 (0.87, 1.44)	1.09 (0.99, 1.20)	1.09 (1.04, 1.16)	1.11 (1.04, 1.18)
Ischemic (102,827)	1.09 (1.04, 1.14)	NA	NA	1.12 (0.77, 1.64)	1.03 (0.92, 1.16)	1.10 (1.03, 1.18)	1.10 (1.02, 1.20)
Cerebrovascular (19,905)	1.16 (1.05, 1.29)	0.12 (0.00, 27.94)	NA	1.12 (0.77, 1.64)	1.27 (0.87, 1.86)	1.21 (1.04, 1.41)	1.10 (0.93, 1.30)
Respiratory (54,494)	1.08 (1.02, 1.15)	0.36 (0.10, 1.36)	1.63 (0.15, 18.28)	0.81 (0.47, 1.37)	1.17 (0.97, 1.40)	1.05 (0.96, 1.14)	1.14 (1.02, 1.28)
Nephritis and nephrotic (4160)	1.03 (0.82, 1.28)	1.83 (0.15, 22.31)	NA	1.60 (0.34, 7.85)	0.75 (0.40, 1.42)	1.04 (0.75, 1.45)	1.09 (0.76, 1.57)
Acute Renal Failure (684)	1.14 (0.66, 2.00)	NA	NA	NA	0.75 (0.40, 1.42)	0.87 (0.39, 1.91)	1.09 (0.76, 1.57)
Mental Disorders (12,108)	1.02 (0.90, 1.17)	NA	NA	0.80 (0.43, 1.49)	0.89 (0.60, 1.32)	1.08 (0.86, 1.37)	1.05 (0.87, 1.27)

Results are pooled across all climate divisions using fixed-effects meta-analysis. Bold values indicate 95% CIs that did not include 1.

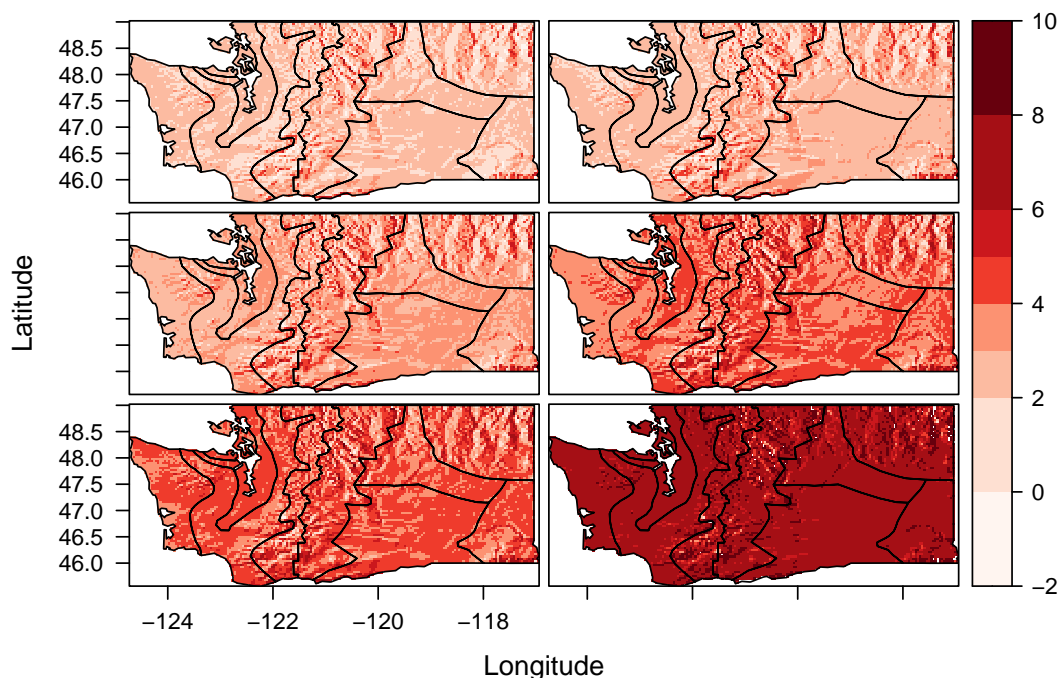


Figure 4. Spatial distribution of projected humidex anomalies. Columns denote RCPs: left is RCP4.5, right is RCP8.5; rows indicate years: top is 2030, middle is 2050, and bottom is 2080.

Table 5. Number of deaths attributable to heat above the 99th percentile of humidex in the historical period and projected percent increase due to climate change.

Climate Division	Historical (N)	Percent Increase					
		2030		2050		2080	
		RCP4.5	RCP8.5	RCP4.5	RCP8.5	RCP4.5	RCP8.5
Cascade Mountains West	2	0	100	100	200	200	900
Central Basin	25	32	68	112	224	252	1156
E Olympic Cascade Foothills	61	11	28	57	133	152	556
E Slope Cascades	1	100	100	100	200	200	1100
NE Olympic San Juan	21	43	62	119	238	252	1652
Northeastern	33	42	76	124	245	276	1306
Okanogan Big Bend	3	33	33	100	200	233	1067
Palouse Blue Mountains	1	100	200	300	500	700	2900
Puget Sound Lowlands	283	23	42	87	178	196	812
West Olympic Coast	6	0	0	33	100	133	617

Bold rows indicate climate divisions where 95% CIs did not include 0.

The percent increases in Table 5 reflect the warming patterns given in Figure 4. In each year, the percent increase of attributable heat deaths is higher under RCP8.5 than RCP4.5, and the discrepancy between the two greenhouse gas concentrations scenarios increases with time. Of the three climate divisions with statistically significant results, NE Olympic San Juan is projected to have the greatest increase in deaths attributable to heat (values range from 43% in 2030 under RCP 4.5 to 1652% in 2080 under RCP8.5), whereas E Olympic Cascade Foothills has the smallest projected percent increase (values range from 11% to 556%). Across these three climate divisions, the average percent increase in heat-attributable deaths is 35%, 135%, and 603% in 2030, 2050, and 2080, respectively.

4. Discussion

This study used a case-crossover analysis to describe the historical relationship between heat and non-traumatic mortality in Washington’s ten climate divisions. Fixed-effects meta-analysis was used to simplify the exposure–response curves to a single, state-wide

value, the OR of non-traumatic mortality at the 99th percentile of humidex compared to the 50th percentile. Subgroup analyses were also conducted to investigate effect modification by age, sex, race/ethnicity, and cause of death. Finally, the historical exposure–response curves were combined with climate projections to investigate the impact of climate change on an existing public health issue. The results provide evidence that high values of humidex are associated with increased non-traumatic mortality in Washington and indicate that climate change could lead to an increased number of deaths attributable to extreme heat.

The state-wide OR value produced in this study was 1.08 (1.06, 1.10). This value for risk of mortality associated with same-day heat events is quite similar to results from Seattle [28,36] and King County [8] as well as Sydney, Australia [19], South Korea [56], and Sweden [13]. However, it is less than risk estimates produced in southern Europe [11,12] and greater than values from other parts of the United States [6,24]; these differences are likely driven by varied access to air conditioning or levels of physiological acclimatization.

The J- and U-shaped dose–response curves in Figure 2 are characteristic of the relationship between heat and mortality [2,3] and indicate elevated risks of mortality at high values of humidex (for J-shaped curves) or both low and high values of humidex (for U-shaped curves). Busch Isaksen and colleagues [7,8] previously described a J-shaped curve for King County and identified 30 humidex as the value at which risk of mortality increases. The East Olympic Cascade Foothills, NE Olympic San Juan, Northeastern, and Puget Sound Lowlands climate divisions are similarly described by an elevated risk threshold of approximately 30 humidex. The consistency of this threshold across climate divisions in Washington may indicate that it is an appropriate “trigger point” for the implementation of strategies that aim to reduce adverse heat-related health events within the state [57]. Notably, this is a lower threshold than used by the National Weather Service to issue heat alerts in other parts of the country [58].

Knowledge about the heat–mortality relationship using climate zones or climate regions rather than geopolitical units has the potential to provide better guidance for policymakers attempting to mitigate heat-related deaths, including through the development of heat warning systems [59,60]. Nevertheless, such an approach is not widespread in studies of heat-related mortality. Guirguis et al. [61] detected a significant increase in hospitalizations during hot weather in comparison to hospitalizations observed over all days, independent of any temperature threshold, in the coastal region of San Diego County, but not in communities further inland that are characterized by higher average temperatures and greater air conditioning prevalence. Regional time series analyses in South Korea [56] as well as regional case-crossover analyses in India [15] also yielded distinct temperature–mortality relationships for different climate regions. However, Basagaña et al. [12] failed to detect heterogeneity in the heat–mortality relationship across Catalonia’s 14 climatic zones, and chose instead to focus on a single meta-analysis. Overall, the spatial results from this study are somewhat mixed. Although the exposure–response curves suggest qualitative differences in the heat–mortality relationship between zones in Washington (Figure 2), the similar ORs comparing 99th to 50th percentiles (Figure 3) may suggest that individuals in the state respond to their differing local temperatures in a similar manner. It is unclear whether the differences in results are due to methodological choices, the region of study, or some other factor, and the use of climate variables to aggregate health outcomes in epidemiological studies remains an emerging area of research with unanswered questions.

Stratified analyses for individual-level characteristics indicate that risk of non-traumatic mortality on 99th percentile days increases with age, particularly in the 85+ age group, and that risk is higher among women than men and among Blacks than other racial/ethnic groups (Table 3). Age is a well-established risk factor for heat-related mortality [4,8,11,14,15]. Greater risk among women has been identified previously in Italy [11] and Spain [12], although conflicting results have been observed in King County, Washington [8] and elsewhere in the U.S. [28,62] as well as in Latin America [14], Russia [18], and South Korea [56], where either men were at greater risk or there was no difference across sexes. An area for future research is to elucidate the cause of these conflicting results, e.g., differences in study demo-

graphics or methodology. The disparities across racial groups are consistent with previous studies [23–25,28] and are likely due to socioeconomic differences across racial groups perpetuated by institutionalized racism [25,29,63]. To reiterate, in the context of heat-related mortality, race is best thought of as a *risk marker* rather than a *risk factor* [64], or a *social construct* rather than a *biological determinant* [63]. Nevertheless, the results stratified by race/ethnicity are useful because they can help to inform the allocation of medical/public health resources [65,66].

Diabetic, circulatory, cardiovascular, ischemic, cerebrovascular, and respiratory deaths are also significantly associated with heat (Table 4). The results for all causes of death except for ischemic are largely consistent with previous results [6,8,12,13,22,23], although Busch Isaksen and colleagues [8] did not obtain a significant association for respiratory deaths. A significant association for ischemic deaths is consistent with Wilson et al. [19] but contradicts other existing work [8,15]. Finally, null results for nephritis and nephrotic, acute renal failure and mental disorder deaths mostly agree with prior research [8,19], although Basagaña et al. [12] found significant results for mental disorders. Explaining these contrasting results for certain causes of death is a potential area for future research.

The projected heat-attributable deaths are higher than the historical value in almost every climate division under both RCP4.5 and RCP8.5 and in 2030, 2050, and 2080 (Table 5). The direction of this result agrees with most existing studies, despite different study areas and methodological choices [9,62,67–69]. In the Puget Sound Lowlands, there were an average of 7.3 annual heat-related deaths in the historical period, almost identical to the value of 7.1 obtained by Busch Isaksen et al. [7] for King County. However, it is difficult to compare projections from this study directly to results from Busch Isaksen et al. [7], as different methodologies were used, and, consequently, the magnitude of the projected values represents different quantities. The approach used by Jackson et al. [36] is more similar to this study, and the results are identical qualitatively (increase in heat-related mortality over the historical period, a gap between warming scenarios/RCPs that grows with time, and results that are statistically significant only in the western part of the state) and similar quantitatively (large increase under moderate warming/RCP4.5 and drastic increase under high warming/RCP8.5).

Projected increases in heat-attributable mortality in the New York City region in 2050 [67] as well as select American metropolitan areas in both 2050 and 2090 [62] are lower than results from this study, possibly indicating that Washington is more vulnerable to heat-related mortality in a changing climate than other parts of the country. The projected heat-attributable mortality values are similar in 2030 under RCP4.5 and RCP8.5, but the difference between these scenarios grows with time and is quite large by 2080; the values for 2050 under RCP8.5 are also quite similar to the values for 2080 under RCP4.5. This temporal pattern is consistent with results from Wellenius et al. [62], and Shindell et al. [9] also observed a large discrepancy between these RCPs in the 2090s. In contrast, Guo et al. [69] observed percent increases that were more consistent from one scenario to the next. Overall, the somewhat contrasting results in projected heat-attributable mortality across studies likely stem from different data and methodology, such as the temperature threshold used to calculate the number of heat-attributable deaths.

A case-crossover analysis conducted in Sweden illustrated the importance of incorporating regional information about the heat–mortality relationship when developing public health interventions [13]. Kalkstein et al. [70] argue that a general decline across 40 U.S. cities in mortality rates attributable to extreme heat events since 1996 when compared to rates from 1975–1995—a decline that occurred despite a warming climate—can be attributed, at least in part, to resources related to education, notification, and response measures associated with heat-related health outcomes in many of the 40 cities. Ebi et al. [71] estimate that the Philadelphia Hot Weather-Health Watch/Warning System saved 117 lives during a three-summer period, and Heo et al. [56] attribute lower mortality risk during heat events among the elderly in 2008–2012 compared to 1996–2000 to the introduction of a heatwave forecast system in 2008 that targeted elderly individuals. Therefore, there is precedent for using results similar to the historical analysis in this study to improve

heat-related health outcomes in a changing climate. In contrast to these results from other locations, however, it is possible that heat-related mortality has increased in Seattle over time [72]. Consequently, there is a clear need to incorporate this knowledge into public health decision-making in Washington.

The research design expands upon existing work in Washington [7,8,36] in a number of ways. First, the case-crossover approach is novel in the state. Using this technique was one of the study goals, and it was a beneficial choice because it does not require “denominator” data (i.e., population size), which could be difficult to obtain for Washington’s climate divisions. Previous research in King County, Washington [7,8] has used a Poisson time series model to describe the relationship between humidex and mortality. Notably, studies that have applied both a time series and case-crossover approach assert that the two techniques generate results that are comparable quantitatively and identical qualitatively [73,74]. We confirmed this by using King County to conduct a sensitivity analysis (Figure S1). The major difference between the two approaches is that a case-crossover analysis produces odds ratios, whereas a Poisson time series model produces relative risks. However, Basu, Dominici, and Samet [75] observe that estimates produced with either method are often directly comparable, as mortality is a rare event. Thus, despite the utilization of a different technique, it is possible to compare historical results from this study to results in Busch Isaksen et al. [7,8].

In addition to the use of a novel analytic technique, this study also incorporated data from the entire state of Washington. Previous work has been restricted to King County [7,8] or selected populous areas in the state [36]. The use of data through the year 2018 also resulted in an analysis with a larger historical timeframe than any existing study. Because this study used NOAA’s climate divisions [38] to group deaths, it is the first in Washington to use a form of spatial aggregation not based on geopolitical boundaries. Finally, regarding the projections component of this study, the use of 20 different climate models implicitly accounts for uncertainty in climate model physics, which may be more important in projections of heat-related mortality than uncertainty associated with greenhouse gas emissions [76]. This is a notable improvement over the two existing projections studies in the state [7,36], each of which use only two climate models.

There are a number of limitations to this study. Although humidex exposure was assigned on an individual level using a nearest neighbors calculation, there is still likely to be some exposure misclassification; for example, individuals may be far from their residence on the control days preceding death or even on the date of death itself, so the assigned humidex exposure may not represent conditions that these individuals actually experienced. The price to pay for controlling for temporal confounding using the case-crossover design is reduced statistical efficiency [77]. This was likely demonstrated by only four of the ten climate divisions having statistically significant ORs due to the small sample sizes in some parts of the state. Moreover, it is possible that the choice of a quadratic polynomial is undesirable when applying the dose–response curves to future climate scenarios, as the climate projections contain temperatures outside of the observed historical range and polynomials (when compared to splines) may “misbehave” outside of the range of data used to fit them.

Although other researchers have adjusted for air pollution exposure, this potential confounder was not included in this study for two principal reasons. First, the main interest of this research was the total (and not direct) effect of heat on mortality. Previous work has also failed to identify any significant effect modification by air pollutants [73]. This study also did not incorporate socioeconomic variables, which may be important, as those variables are likely to be highly correlated with access to air conditioning, a documented modifier of the heat–health relationship [5,22,24,61]. Finally, this study may also fail to produce the true heat–mortality curve because it did not include the impact of lagged and/or multi-day exposure. However, a prior analysis in Washington did not detect lagged or multi-day effects, and instead identified mortality effects occurring on the same day as exposure to be most critical [8].

Using areas defined by climatic variables has notable benefits, but the lack of previous work utilizing this method of spatial aggregation, particularly in the Pacific Northwest, complicated direct comparison of effect estimates. Climate is also not the only factor that influences the heat–mortality relationship, so the use of climatological rather than geopolitical aggregation could mask some other important and locally varying factors, such as public health messaging or socioeconomic variables, that influence the heat–mortality relationship. Furthermore, the specific use of climate divisions identified by NOAA may be problematic because the boundaries are not necessarily intended to create areas of climatological homogeneity (instead, the divisions were often based on crop considerations and/or drainage basins), and some divisional boundaries are chosen to coincide with county boundaries [38]. Indeed, on a single day, meteorological variables can vary greatly across a single climate division.

An alternative to NOAA’s climate divisions is the Köppen–Geiger climate classification [78], which was used directly by Fu et al. [15] in India and indirectly by Guirguis et al. [61] in San Diego County. Although this scheme is also based primarily on five distinct vegetation types, each of these major classifications are divided further based on explicitly defined temperature and precipitation ranges. Although there is some microclimate heterogeneity, most of Washington falls into one of three main Köppen–Geiger climate types: areas west of the Cascades are mostly warm temperate climate (C), whereas east of the Cascades is a mix of snowy climates (D) in the northeast and both arid climate (B) and warm temperate climate (C) in the southeast. Interestingly, three of the four climate divisions with significant humidex–mortality exposure–response curves (East Olympic Cascade, NE Olympic San Juan, and Puget Sound Lowlands) lie west of the Cascades and are characterized primarily by warm, temperate climates with dry summers. This region of the state is divided into two sub-types based on precipitation, but it is possible that this division is not important for heat-related mortality and that, for the purposes of public health applications, these three climate divisions should be grouped together. A potential area for future research is to compare the variability of exposure metrics such as humidex within and between climate zones to variability of that meteorological variable within and between counties to assess the validity of using climate divisions for spatial aggregation in the context of heat-related health outcomes.

Independent of the specific boundaries chosen, a problem that will persist is climatological heterogeneity across a single region. This heterogeneity is likely to increase as the size of the region increases and may favor the use of cities or counties for aggregation, as these smaller-scale regions could have less heterogeneity, even if their boundaries are not influenced by climate variables. When appropriate, the optimal approach may be to divide a city or county into climate zones, as in Guirguis et al. [61]; this approach requires both true meteorological heterogeneity across the city/county as well as a spatial distribution of population that allows for the necessary statistical power to ascertain differences from one climate zone to the next. An important area for further research is the use of climatological variables for spatial aggregation when studying heat-related health outcomes as well as the importance of the choice of a specific climate classification.

The second portion of the study, the projected public health burden, incorporated uncertainty in greenhouse gas trajectories by using two different RCPs, but it did not include an aggressive decarbonization scenario (i.e., RCP2.6). This is a notable disadvantage when compared to existing projections in the state [7,36], which include low, moderate, and high warming scenarios. However, more recent work in major U.S. cities [45] and London [55] also include only RCP4.5 and RCP8.5 in their projections, so there is precedent for excluding a low-emission trajectory. There are also limitations associated with the use of bias-corrected climate projections; for example, the downscaled data will inherit any imperfections in the training data [43], and the calibration procedure in Ho et al. [48] specifically may yield an increase in the 99th percentile that is greater than the mean. Additionally, the reported heat-attributable deaths are only for values of humidex above the historical 99th percentile and may not represent the full extent of mortality associated with extreme heat; for instance,

an “optimal alert threshold” in King County has previously been identified as being below the 99th percentile [8].

The study also does not incorporate uncertainty in adaptation scenarios, which may be even greater than the uncertainty associated with climate modeling [79]. Adaptation was not incorporated because it requires arbitrary modeling choices related to the extent and timing of adaptation mechanisms [55]. However, it is likely that adaptation, especially in Washington, a state that historically has had relatively low air conditioning prevalence, would help to mitigate future heat-related mortality below the projected increases. Although the scenarios explored in this study—no adaptation and constant population—are simplistic, they yield projections that have isolated the effect of climate.

A final limitation of the projections component is the use of CMIP5 GCMs, which have been superseded by CMIP6 models. The choice to use CMIP5 was driven by previous work that used these models [45,55]. Nevertheless, it is possible that employing more recent GCMs would have improved the accuracy of the projected heat-related mortality calculations, and future studies would be well served to use the most up-to-date climate projections. In general, little consideration has been given to the implications of the specific climate models used when projecting heat-related mortality, nor how using different and/or outdated models may impact the success of public health initiatives that aim to improve heat-related health outcomes. Comparing projections of heat-related mortality under different climate models—rather than simply under different greenhouse gas trajectories—is a critical area for future research.

Overall, projecting heat-related mortality in Washington State, and the Pacific Northwest broadly, remains an important area of research. During late June and early July 2021, a “heat dome” covered the Pacific Northwest and, according to the Washington State Department of Health, killed 100 people in Washington alone [80]. In other words, a single, long-duration extreme heat event of unprecedented magnitude resulted in nearly 25% as many heat-related deaths as this research identified during the 39 years covered in the historical analysis. If such events become more routine due to climate change, then the projections presented in this study may grossly underestimate the future public health burden of heat-related mortality in Washington, absent any widespread adaptation or acclimatization to high temperatures: even in the most extreme projection (RCP8.5 in 2080), there are only about 67 additional yearly deaths projected for E Olympic Cascade Foothills, NE Olympic San Juan, and Puget Sound Lowlands combined. Therefore, further exploration into the potential frequency of these extremely high-intensity heat events as well as the mitigating capacity of adaptation/acclimatization will yield more realistic projections that can better inform data-driven public health decision-making.

5. Conclusions

By quantifying the impact of exposure to extreme temperatures, policymakers can develop preventative, life-saving measures, warning systems, and action plans that target susceptible groups, support health systems, and engage the community at large [81,82]. The application of a novel quantitative method and spatial unit of aggregation combined with contemporary data that span the entire state has provided further evidence that heat-related mortality is an extant public health problem in Washington, particularly among age categories 45–64, 65–84, and 85+ years of age; and for diabetic, circulatory, cardiovascular, ischemic, cerebrovascular, and respiratory causes of deaths. This study provides evidence that our projected climate under two future scenarios will exacerbate extreme heat–mortality risk, especially for communities residing in the E Olympic Cascade Foothills, NE Olympic San Juan, and Puget Sound Lowlands climate zones. The recent June/July 2021 “heat dome”—and the high number of deaths associated with this event [80]—may foreshadow the future of Washington in the absence of meaningful action to combat climate change and prepare for the accompanying public health crisis of heat-related mortality. However, by following the successes observed in other locations, the results of this study

can help inform initiatives and adaptations within Washington that aim to improve heat-related health outcomes and ameliorate the challenges imposed by a changing climate.

Supplementary Materials: The following supporting information can be downloaded at: www.mdpi.com/xxx/s1, Table S1: AIC values for conditional logistic regression models using polynomials between degrees 2 and 10 for each climate division; Table S2: Odds ratio (95% CI) of non-traumatic mortality comparing the 99th and 50th percentiles of humidex, for ages 0–4 and for each climate division; Table S3: Odds ratio (95% CI) of non-traumatic mortality comparing the 99th and 50th percentiles of humidex, for ages 5–14 and for each climate division; Table S4: Odds ratio (95% CI) of non-traumatic mortality comparing the 99th and 50th percentiles of humidex, for ages 15–44 and for each climate division; Table S5: Odds ratio (95% CI) of non-traumatic mortality comparing the 99th and 50th percentiles of humidex, for ages 45–64 and for each climate division; Table S6: Odds ratio (95% CI) of non-traumatic mortality comparing the 99th and 50th percentiles of humidex, for ages 65–84 and for each climate division; Table S7: Odds ratio (95% CI) of non-traumatic mortality comparing the 99th and 50th percentiles of humidex, for ages 85+ and for each climate division; Table S8: Odds ratio (95% CI) of non-traumatic mortality comparing the 99th and 50th percentiles of humidex, for males pooled across all climate divisions; Table S9: Odds ratio (95% CI) of non-traumatic mortality comparing the 99th and 50th percentiles of humidex, for females pooled across all climate divisions; Table S10: Odds ratio (95% CI) of non-traumatic mortality comparing the 99th and 50th percentiles of humidex, by race/ethnicity for each climate division; Table S11: Odds ratio (95% CI) of non-traumatic mortality comparing the 99th and 50th percentiles of humidex, for each racial/ethnic category by age, sex, and cause of death; Figure S1: Humidex–mortality exposure–response curves for King County, produced using both a case-crossover analysis and a time series analysis; Figure S2: The number of days each year where the average climate zone-level humidex exceeds the 99th percentile.

Author Contributions: Conceptualization, L.A. and T.B.I.; methodology, L.A. and M.D.S.; software, L.A.; formal analysis, L.A.; resources, T.B.I.; writing—original draft preparation, L.A.; writing—review and editing, M.D.S. and T.B.I.; visualization, L.A.; supervision, T.B.I. All authors have read and agreed to the published version of the manuscript.

Funding: This research was completed in partial fulfillment of the requirements to obtain the Master of Science degree in the Quantitative Ecology and Resource Management (QERM) graduate program at the University of Washington. Funding for this research came directly from the QERM program and is not tied to any specific grant or research requirements. The QERM program was not involved in the development of this research. This research did not receive any specific grant from funding agencies in the public, commercial, or not-for-profit sectors.

Institutional Review Board Statement: According to the Washington State Institutional Review Board, the use of Washington State mortality data are exempt from review, and, therefore, an application for official exempt status review is not needed.

Informed Consent Statement: Not Applicable.

Data Availability Statement: Restrictions apply to the availability of some data included in this study. Mortality data was obtained from the Washington State Department of Health (WA DOH) and are available at <https://doh.wa.gov/data-statistical-reports/washington-tracking-network-wtn/death> (accessed on 30 May 2022) with the permission of the WA DOH. Historical meteorological data and climate projection data were both obtained from the University of California Merced Climatology Lab and are available for download at <https://www.climatologylab.org/gridmet.html> (accessed on 30 May 2022) and <https://www.climatologylab.org/maca.html> (accessed on 30 May 2022), respectively.

Acknowledgments: This article has been contributed to by US Government employees and their work is in the public domain in the USA. Any use of trade, firm, or product names is for descriptive purposes only and does not imply endorsement by the U.S. Government.

Conflicts of Interest: The authors declare no conflict of interest.

References

1. Kilbourne, E.M. Heat Waves and Hot Environments. In *The Public Health Consequences of Disasters*; Noji, E.K., Ed.; Oxford University Press: New York, NY, USA, 1997; pp. 245–269.
2. Basu, R.; Samet, J.M. Relation Between Elevated Ambient Temperature and Mortality: A Review of the Epidemiologic Evidence. *Epidemiol. Rev.* **2002**, *24*, 190–202. [[CrossRef](#)]
3. Gosling, S.N.; Lowe, J.A.; McGregor, G.R.; Pelling, M.; Malamud, B.D. Associations Between Elevated Atmospheric Temperature and Human Mortality: A Critical Review of the Literature. *Clim. Chang.* **2009**, *92*, 299–341. [[CrossRef](#)]
4. Kalkstein, L.S.; Davis, R.E. Weather and Human Mortality: An Evaluation of Demographic and Interregional Responses in the United States. *Ann. Assoc. Am. Geogr.* **1989**, *79*, 44–64. [[CrossRef](#)]
5. Curriero, F.C.; Heiner, K.S.; Samet, J.M.; Zeger, S.L.; Strug, L.; Patz, J.A. Temperature and Mortality in 11 Cities of the Eastern United States. *Am. J. Epidemiol.* **2002**, *155*, 80–87. [[CrossRef](#)]
6. Medina-Ramón, M.; Schwartz, J. Temperature, Temperature Extremes, and Mortality: A Study of Acclimatisation and Effect Modification in 50 US Cities. *Occup. Environ. Med.* **2007**, *64*, 827–833. [[CrossRef](#)]
7. Busch Isaksen, T.; Yost, M.; Hom, E.; Fenske, R. Projected Health Impacts of Heat Events in Washington State Associated with Climate Change. *Rev. Environ. Health* **2014**, *29*, 119–123.
8. Isaksen, T.B.; Fenske, R.A.; Hom, E.K.; Ren, Y.; Lyons, H.; Yost, M.G. Increased Mortality Associated with Extreme-Heat Exposure in King County, Washington, 1980–2010. *Int. J. Biometeorol.* **2015**, *60*, 85–98. [[CrossRef](#)]
9. Shindell, D.; Zhang, Y.; Scott, M.; Ru, M.; Stark, K.; Ebi, K.L. The Effects of Heat Exposure on Human Mortality Throughout the United States. *Geohealth* **2020**, *4*, e2019GH000234. [[CrossRef](#)] [[PubMed](#)]
10. Weinberger, K.R.; Harris, D.; Spangler, K.R.; Zanobetti, A.; Wellenius, G.A. Estimating the Number of Excess Deaths Attributable to Heat in 297 United States Counties. *Environ. Epidemiol.* **2020**, *4*, e096. [[CrossRef](#)] [[PubMed](#)]
11. Stafoggia, M.; Forastiere, F.; Agostini, D.; Biggeri, A.; Bisanti, L.; Cadum, E.; Caranci, N.; de’Donato, F.; De Lisio, S.; De Maria, M.; et al. Vulnerability to Heat-Related Mortality: A Multicity, Population-Based, Case-Crossover Analysis. *Epidemiology* **2006**, *17*, 315–323. [[CrossRef](#)] [[PubMed](#)]
12. Basagaña, X.; Sartini, C.; Barrera-Gómez, J.; Dadvand, P.; Cunillera, J.; Ostro, B.; Sunyer, J.; Medina-Ramón, M. Heat Waves and Cause-Specific Mortality at All Ages. *Epidemiology* **2011**, *22*, 765–772. [[CrossRef](#)] [[PubMed](#)]
13. Åström, D.O.; Åström, C.; Forsberg, B.; Vicedo-Cabrera, A.M.; Gasparrini, A.; Oudin, A.; Sundquis, K. Heat Wave-Related Mortality in Sweden: A Case-Crossover Study Investigating Effect Modification by Neighbourhood Deprivation. *Scand. J. Public Health* **2020**, *48*, 6.
14. Bell, M.L.; O’Neill, M.S.; Ranjit, N.; Borja-Aburto, V.H.; Cifuentes, L.A.; Gouveia, N.C. Vulnerability to Heat-Related Mortality in Latin America: A Case-Crossover Study in São Paulo, Brazil, Santiago, Chile and Mexico City, Mexico. *Int. J. Epidemiol.* **2008**, *37*, 796–804. [[CrossRef](#)]
15. Fu, S.H.; Gasparrini, A.; Rodriguez, P.S.; Jha, P. Mortality Attributable to Hot and Cold Ambient Temperatures in India: A Nationally Representative Case-Crossover Study. *PLoS Med.* **2018**, *15*, e1002619. [[CrossRef](#)]
16. Dimitrova, A.; Ingole, V.; Basagaña, X.; Ranzani, O.; Milà, C.; Ballester, J.; Tonne, C. Association between ambient temperature and heat waves with mortality in South Asia: Systematic review and meta-analysis. *Environ. Int.* **2021**, *146*, 106170. [[CrossRef](#)] [[PubMed](#)]
17. Guo, Y.; Barnett, A.G.; Pan, X.; Yu, W.; Tong, S. The Impact of Temperature on Mortality in Tianjin, China: A Case-Crossover Design with a Distributed Lag Nonlinear Model. *Environ. Health Perspect.* **2011**, *119*, 1719–1725. [[CrossRef](#)]
18. Shaposhnikov, D.; Revich, B.; Bellander, T.; Bedada, G.B.; Bottai, M.; Kharkova, T.; Kvasha, E.; Lezina, E.; Lind, T.; Semutnikova, E.; et al. Mortality Related to Air Pollution with the Moscow Heat Wave and Wildfire of 2010. *Epidemiology* **2014**, *25*, 359–364. [[CrossRef](#)]
19. Wilson, L.A.; Morgan, G.G.; Hanigan, I.C.; Johnston, F.H.; Abu-Rayya, H.; Broome, R.; Gaskin, C.; Jalaludin, B. The Impact of Heat on Mortality and Morbidity in the Greater Metropolitan Sydney Region: A Case Crossover Analysis. *Environ. Health* **2013**, *12*, 98. [[CrossRef](#)] [[PubMed](#)]
20. Wichmann, J. Heat effects of ambient apparent temperature on all-cause mortality in Cape Town, Durban and Johannesburg, South Africa: 2006–2010. *Sci. Total Environ.* **2017**, *587–588*, 266–272. [[CrossRef](#)]
21. Ahmadalipour, A.; Moradkhani, H. Escalating heat-stress mortality risk due to global warming in the Middle East and North Africa (MENA). *Environ. Int.* **2018**, *117*, 215–225. [[CrossRef](#)]
22. Semenza, J.C.; Ruin, C.H.; Falter, K.H.; Selanikio, J.D.; Flanders, W.D.; Howe, H.L.; Wilhelm, J.L. Heat-Related Deaths During the July 1995 Heat Wave in Chicago. *N. Engl. J. Med.* **1996**, *335*, 84–90. [[CrossRef](#)] [[PubMed](#)]
23. Schwartz, J. Who Is Sensitive to Extremes of Temperature? A Case-Only Analysis. *Epidemiology* **2005**, *16*, 67–72. [[CrossRef](#)] [[PubMed](#)]
24. O’Neill, M.S.; Zanobetti, A.; Schwartz, J. Disparities by Race in Heat-Related Mortality in Four US Cities: The Role of Air Conditioning Prevalence. *J. Urban Health* **2005**, *82*, 191–197. [[CrossRef](#)]
25. Madrigano, J.; Lane, K.; Petrovic, N.; Ahmed, M.; Blum, M.; Matte, T. Awareness, Risk Perception, and Protective Behaviors for Extreme Heat and Climate Change in New York City. *Int. J. Environ. Res. Public Health* **2018**, *15*, 1433. [[CrossRef](#)]
26. Gravlee, C.C. How Race Becomes Biology: Embodiment of Social Inequality. *Am. J. Phys. Anthropol.* **2009**, *129*, 47–57. [[CrossRef](#)]

27. Boyd, R.W.; Lindo, E.G.; Weeks, L.D.; McLemore, M.R. On Racism: A New Standard for Publishing on Racial Health Inequities. *Health Affairs Blog* **2020**, *10*, 1.
28. O'Neill, M.S.; Zanobetti, A.; Schwartz, J. Modifiers of the Temperature and Mortality Association in Seven US Cities. *Am. J. Epidemiol.* **2003**, *157*, 1074–1082. [[CrossRef](#)]
29. Hoffman, J.S.; Shandas, V.; Pendleton, N. The Effects of Historical Housing Policies on Resident Exposure to Intra-Urban Heat: A Study of 108 US Urban Areas. *Climate* **2020**, *8*, 12. [[CrossRef](#)]
30. Cissé, G.; McLeman, R.; Adams, H.; Aldunce, P.; Bowen, K.; Campbell-Lendrum, D.; Clayton, S.; Ebi, K.L.; Hess, J.; Huang, C.; et al. Health, Wellbeing, and the Changing Structure of Communities. Contribution of Working Group II to the Sixth Assessment Report of the Intergovernmental Panel on Climate Change. In *Climate Change 2022: Impacts, Adaptation, and Vulnerability*; Pörtner, H.-O., Roberts, D.C., Tignor, M., Poloczanska, E.S., Mintenbeck, K., Alegría, A., Craig, M., Langsdorf, S., Lösschke, S., Möller, V., et al., Eds.; Cambridge University Press: Cambridge, UK; New York, NY, USA, 2022; pp. 5–6, *in press*
31. Kalkstein, L.S.; Greene, J.S. An Evaluation of Climate/Mortality Relationships in Large u.s. Cities and the Possible Impacts of a Climate Change. *Environ. Health Perspect.* **1997**, *105*, 84–93. [[CrossRef](#)]
32. Reid, C.E.; O'Neill, M.S.; Gronlund, C.J.; Brines, S.J.; Brown, D.G.; Diez-Roux, A.V.; Schwartz, J. Mapping Community Determinants of Heat Vulnerability. *Environ. Health Perspect.* **2009**, *117*, 1730–1736. [[CrossRef](#)]
33. Sheridan, S.C.; Kalkstein, A.J. Seasonal Variability in Heat- Related Mortality Across the United States. *Nat. Hazards* **2010**, *55*, 291–305. [[CrossRef](#)]
34. IPCC. *Climate Change 2013: The Physical Science Basis. Contribution of Working Group 1 to the Fifth Assessment Report of the Intergovernmental Panel on Climate Change*; Stocker, T.F., Qin, D., Plattner, G.-K., Tignor, M., Allen, S.K., Boschung, J., Nauels, A., Xia, Y., Bex, V., Midgley, P.M., Eds.; Cambridge University Press: Cambridge, UK; New York, NY, USA, 2013.
35. Meehl, G.A.; Tebaldi, C. More Intense, More Frequent, and Longer Lasting Heat Waves in the 21st Century. *Science* **2004**, *13*, 994–997. [[CrossRef](#)] [[PubMed](#)]
36. Jackson, J.E.; Yost, M.G.; Karr, C.; Fitzpatrick, C.; Lamb, B.K.; Chung, S.H.; Avise, J.; Rosenblatt, R.A.; Fenske, R.A. Public Health Impacts of Climate Change in Washington State: Projected Mortality Risks Due to Heat Events and Air Pollution. *Clim. Chang.* **2010**, *102*, 159–186. [[CrossRef](#)]
37. Šeparović, L.; Alexandru, A.; Laprise, R.; Martynov, A.; Sushama, L.; Winger, K.; Tete, K.; Valin, M. Present Climate and Climate Change over North America as Simulated by the Fifth-Generation Canadian Regional Climate Model. *Clim. Dyn.* **2013**, *41*, 3167–3201. [[CrossRef](#)]
38. Guttman, N.B.; Quayle, R.G. A Historical Perspective of US Climate Divisions. *Bull. Am. Meteorol. Soc.* **1996**, *77*, 293–303. [[CrossRef](#)]
39. Abatzoglou, J.T. Development of Gridded Surface Meteorological Data for Ecological Applications and Modelling. *Int. J. Climatol.* **2013**, *33*, 121–131. [[CrossRef](#)]
40. University of California Merced Climatology Lab: gridMET. Available online: <https://www.climatologylab.org/gridmet.html> (accessed on 24 July 2022).
41. Mitchell, K.E.; Lohmann, D.; Houser, P.R.; Wood, E.F.; Schaake, J.C.; Robock, A.; Cosgrove, B.A.; Sheffield, J.; Duan, Q.; Luo, L.; et al. The Multi-Institution North American Land Data Assimilation System (NLDAS): Utilizing Multiple GCIP Products and Partners in a Continental Distributed Hydrological Modeling System. *J. Geophys. Res. Atmos.* **2004**, *109*, D07S90. [[CrossRef](#)]
42. Daly, C.; Halbleib, M.; Smith, J.I.; Gibson, W.P.; Doggett, M.K.; Taylor, G.H.; Curtis, J.; Pasteris, P.A. Physiographically-Sensitive Mapping of Temperature and Precipitation Across the Conterminous United States. *Int. J. Climatol.* **2008**, *28*, 2031–2064. [[CrossRef](#)]
43. Abatzoglou, J.T.; Brown, T.J. A Comparison of Statistical Downscaling Methods Suited for Wildfire Applications. *Int. J. Climatol.* **2011**, *32*, 772–780. [[CrossRef](#)]
44. University of California Merced Climatology Lab: MACA. Available online: <https://www.climatologylab.org/maca.html> (accessed on 24 July 2022).
45. Weinberger, K.R.; Haykin, L.; Eliot, M.N.; Schwartz, J.D.; Gasparrini, A.; Wellenius, G.A. Projected Temperature-Related Deaths in Ten Large u.s. Metropolitan Areas Under Different Climate Change Scenarios. *Environ. Int.* **2017**, *107*, 196–204. [[CrossRef](#)] [[PubMed](#)]
46. Masterton, J.M.; Richardson, F.A. *Humidex; a Method of Quantifying Human Discomfort Due to Excessive Heat and Humidity*; Environment Canada: Downsview, ON, Canada, 1979.
47. Davis, R.E.; McGregor, G.R.; Enfield, K.B. Humidity: A Review and Primer on Atmospheric Moisture and Human Health. *Environ. Res.* **2016**, *144*, 106–116. [[CrossRef](#)]
48. Ho, C.K.; Stephenson, D.B.; Collins, M.; Ferro, C.A.T.; Brown, S.J. Calibration Strategies: A Source of Additional Uncertainty in Climate Change Projections. *Bull. Am. Meteorol. Soc.* **2012**, *93*, 21–26. [[CrossRef](#)]
49. Maclure, M. The Case-Crossover Design: A Method for Studying Transient Effects on the Risk of Acute Events. *Am. J. Epidemiol.* **1991**, *133*, 144–153. [[CrossRef](#)] [[PubMed](#)]
50. Jaakkola, J.J. Case-Crossover Design in Air Pollution Epidemiology. *Eur. Respir. J. Suppl.* **2003**, *40*, 81s–85s. [[CrossRef](#)] [[PubMed](#)]
51. Sheppard, J.H.; Lumley, T. Overlap Bias in the Case-Crossover Design, with Application to Air Pollution Exposures. *Stat. Med.* **2005**, *24*, 285–300.
52. R Core Team. *R: A Language and Environment for Statistical Computing*; R Foundation for Statistical Computing: Vienna, Austria, 2019.

53. Therneau, T.M. A Package for Survival Analysis in R. R Package Version 3.2-3. 2020. Available online: <https://CRAN.R-project.org/package=survival> (accessed on 30 May 2022).
54. Balduzzi, S.; Rücker, G.; Schwarzer, G. How to Perform a Meta-Analysis with R: A Practical Tutorial. *Evid.-Based Ment. Health* **2019**, *22*, 153–160. [[CrossRef](#)]
55. Vicedo-Cabrera, A.M.; Sera, F.; Gasparrini, A. Hands-on Tutorial on a Modeling Framework for Projections of Climate Change Impacts on Health. *Epidemiology* **2019**, *30*, 321–329. [[CrossRef](#)]
56. Heo, S.; Lee, E.; Kwon, B.Y.; Lee, S.; Jo, K.H.; Kim, J. Long-Term Changes in the Heat–Mortality Relationship According to Heterogeneous Regional Climate: A Time-Series Study in South Korea. *BMJ Open* **2016**, *6*, e011786. [[CrossRef](#)] [[PubMed](#)]
57. Petitti, D.; Hodula, D.; Yang, S.; Harlan, S.; Chowell, G. Multiple Trigger Points for Quantifying Heat-Health Impacts: New Evidence from a Hot Climate. *Environ. Health Perspect.* **2016**, *124*, 176–183. [[CrossRef](#)]
58. Weinberger, K.; Zanobetti, A.; Schwartz, J.; Wellenius, G. Effectiveness of National Weather Service heat alerts in preventing mortality in 20 US cities. *Environ. Int.* **2018**, *116*, 30–38. [[CrossRef](#)] [[PubMed](#)]
59. Vaidyanathan, A.; Saha, S.; Vicedo-Cabrera, A.M.; Gasparrini, A.; Abdurehman, N.; Jordan, R.; Hawkins, M.; Hess, J.; Elixhauser, A. Assessment of Extreme Heat and Hospitalizations to Inform Early Warning Systems. *Proc. Natl. Acad. Sci. USA* **2019**, *116*, 5420–5427. [[CrossRef](#)] [[PubMed](#)]
60. McElroy, S.; Schwarz, L.; Green, H.; Corcos, I.; Guirguis, K.; Gershunov, A.; Benmarhnia, T. Defining Heat Waves and Extreme Heat Events Using Sub-Regional Meteorological Data to Maximize Benefits of Early Warning Systems to Population Health. *Sci. Total Environ.* **2020**, *721*, 137678. [[CrossRef](#)] [[PubMed](#)]
61. Guirguis, K.; Basu, R.; Al-Delaimy, W.K.; Benmarhnia, T.; Clemesha, R.E.S.; Corcos, I.; Guzman-Morales, J.; Hailey, B.; Small, I.; Tardy, A.; et al. Heat, Disparities, and Health Outcomes in San Diego County’s Diverse Climate Zones. *Geohealth* **2018**, *2*, 212–223. [[CrossRef](#)]
62. Wellenius, G.A.; Eliot, M.N.; Bush, K.F.; Holt, D.; Lincoln, R.A.; Smith, A.E.; Gold, J. Heat-Related Morbidity and Mortality in New England: Evidence for Local Policy. *Environ. Res.* **2017**, *156*, 845–853. [[CrossRef](#)]
63. Jones, C.P. Invited Commentary: “Race,” Racism, and the Practice of Epidemiology. *Am. J. Epidemiol.* **2001**, *154*, 299–306. [[CrossRef](#)] [[PubMed](#)]
64. Kaplan, J.B.; Bennett, T. Use of Race and Ethnicity in Biomedical Publication. *JAMA* **2003**, *289*, 2709–2716. [[CrossRef](#)] [[PubMed](#)]
65. Kaufman, J.S.; Cooper, R.S. Commentary: Considerations for Use of Racial/Ethnic Classification in Etiologic Research. *Am. J. Epidemiol.* **2001**, *154*, 291–298. [[CrossRef](#)]
66. Bhopal, R. Race and Ethnicity: Responsible Use from Epidemiological and Public Health Perspectives. *J. Law Med. Ethics* **2006**, *34*, 500–507. [[CrossRef](#)]
67. Knowlton, K.; Lynn, B.; Goldberg, R.A.; Rosenzweig, C.; Hogrefe, C.; Rosenthal, J.K.; Kinney, P.L. Projecting Heat-Related Mortality Impacts Under a Changing Climate in the New York City Region. *Am. J. Public Health* **2007**, *97*, 2028–2034. [[CrossRef](#)]
68. Huang, C.; Barnett, A.G.; Wang, X.; Vaneckova, P.; FitzGerald, G.; Tong, S. Projecting Future Heat-Related Mortality Under Climate Change Scenarios: A Systematic Review. *Environ. Health Perspect.* **2011**, *119*, 1681–1690. [[CrossRef](#)]
69. Guo, Y.; Gasparrini, A.; Li, S.; Sera, F.; Vicedo-Cabrera, A.M.; de Sousa Zanotti Stagliorio Coelho, M.; Saldiva, P.H.N.; Lavigne, E.; Tawatsupa, B.; Punnasiri, K.; et al. Quantifying Excess Deaths Related to Heatwaves Under Climate Change Scenarios: A Multicountry Time Series Modelling Study. *PLoS Med.* **2018**, *15*, e1002629. [[CrossRef](#)] [[PubMed](#)]
70. Kalkstein, L.S.; Greene, S.; Mills, D.M.; Samenow, J. An Evaluation of the Progress in Reducing Heat-Related Human Mortality in Major u.s. Cities. *Nat. Hazards* **2011**, *56*, 113–129. [[CrossRef](#)]
71. Ebi, K.L.; Teisberg, T.J.; Kalkstein, L.S.; Robinson, L.; Weiher, R.F. Heat Watch/Warning Systems Save Lives: Estimated Costs and Benefits for Philadelphia 1995–98. *Bull. Am. Meteor. Soc.* **2004**, *85*, 1067–1074. [[CrossRef](#)]
72. Davis, R.E.; Knappenberger, P.C.; Michales, P.J.; Novicoff, W.M. Changing Heat-Related Mortality in the United States. *Environ. Health Perspect.* **2003**, *111*, 1712–1718. [[CrossRef](#)]
73. Zanobetti, A.; Schwartz, J. Temperature and Mortality in Nine US Cities. *Epidemiology* **2008**, *19*, 563–570. [[CrossRef](#)]
74. Tong, S.; Wang, X.Y.; Guo, Y. Assessing the Short-Term Effects of Heatwaves on Mortality and Morbidity in Brisbane, Australia: Comparison of Case-Crossover and Time Series Analyses. *PLoS ONE* **2012**, *7*, e37500. [[CrossRef](#)]
75. Basu, R.; Dominici, F.; Samet, J.M. Temperature and Mortality Among the Elderly in the United States: A Comparison of Epidemiologic Methods. *Epidemiology* **2005**, *16*, 58–66. [[CrossRef](#)]
76. Gosling, S.N.; McGregor, G.R.; Lowe, J.A. The Benefits of Quantifying Climate Model Uncertainty in Climate Change Impacts Assessment: An Example with Heat-Related Mortality Change Estimates. *Clim. Chang.* **2012**, *112*, 217–231. [[CrossRef](#)]
77. Bateson, T.F.; Schwartz, J. Control for Seasonal Variation and Time Trend in Case-Crossover Studies of Acute Effects of Environmental Exposures. *Epidemiology* **1999**, *10*, 539–544. [[CrossRef](#)]
78. Kotttek, M.; Grieser, J.; Beck, C.; Rudolf, B.; Rubel, F. World Map of the köppen-Geiger Climate Classification Updated. *Meteorol. Z.* **2006**, *15*, 259–263. [[CrossRef](#)]
79. Gosling, S.N.; Hondula, D.M.; Bunker, A.; Ibarreta, D.; Liu, J.; Zhang, X.; Sauerborn, R. Adaptation to Climate Change: A Comparative Analysis of Modeling Methods for Heat-Related Mortality. *Environ. Health Perspect.* **2017**, *125*, 087008. [[CrossRef](#)]
80. Washington State Department of Health. Available online: <https://doh.wa.gov/emergencies/be-prepared-be-safe/severe-weather-and-natural-disasters/hot-weather-safety/heat-wave-2021> (accessed on 30 May 2022).

81. Lowe, D.; Ebi, K.L.; Forsberg, B. Heatwave Early Warning Systems and Adaptation Advice to Reduce Human Health Consequences of Heatwaves. *Int. J. Environ. Res. Public Health* **2011**, *8*, 4623–4648. [[CrossRef](#)] [[PubMed](#)]
82. Casanueva, A.; Burgstall, A.; Kotlarski, S.; Messeri, A.; Morabito, M.; Flouris, A.D.; Nybo, L.; Spirig, C.; Schwierz, C. Overview of Existing Heat-Health Warning Systems in Europe. *Int. J. Environ. Res. Public Health* **2019**, *16*, 2657. [[CrossRef](#)] [[PubMed](#)]